The Crystal Structure of Acridinium Bis(7,7,8,8-Tetracyanoquinodimethanide), $ARD^+(TCNQ)_2^-$ and Some Remarks on the Possibility of a Peierls Distortion of a Linear Chain of TCNQ

Hayao KOBAYASHI

Department of Chemistry, Faculty of Science, Toho University, Narashino, Chiba 275

(Received December 10, 1973)

Crystals of acridinium-TCNQ(ARD(TCNQ)$_2$) are triclinic, space group $P\bar{1}$ with $a=3.841(2)$, $b=13.018(6)$, $c=18.370(12)$ Å, $\alpha=114.32(5)$, $\beta=119.31(4)$, $\gamma=90.57(7)°$ and $Z=1$. ARD and TCNQ are separately stacked to form columns along the a axis. Each ARD column is surrounded by six TCNQ columns. The orientation of ARD is disordered. Intermolecular distance between adjacent TCNQs is 3.246 Å and that between adjacent ARDs is 3.418 Å. The possibility of a Peierls distortion of TCNQ columns was discussed on the basis of the model of one-dimensional distorted lattice. Calculations of free energy show that alternation of intermolecular spacing disappears at Peierls transition temperature, T_p of about 200 K. For $T>T_p$, the one-dimensional band is not split (metallic), while it is split below T_p(semiconductive). The specific heat curve shows a peak at about 180 K and the heat of transition is calculated to be about 130 cal/mol.

The recent reports on the extraordinarily high conductivity of TTF–TCNQ[1] ($\sigma>10^4(\Omega\ cm)^{-1}$(60 K)) shed light on the physical basis of the conduction mechanism of TCNQ salts. Besides TTF–TCNQ, three TCNQ salts have been known, whose temperature dependence of the electrical conductivities shows their metallic nature. They are *N*-methylphenazinium-TCNQ (NMP–TCNQ)[2], quinolinium–$TCNQ_2$ (Q(TCNQ)$_2$) and acridinium–$TCNQ_2$(ARD(TCNQ)$_2$)[3,4].

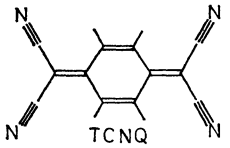

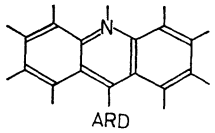

Crystals of ARD(TCNQ)$_2$ were subjected to X-ray crystal structure analysis to obtain structural information. A simple calculation was made to examine the possibility of a Peierls distortion of TCNQ columns.

Experimental

The crystals of ARD(TCNQ)$_2$ were prepared by a diffusion method, an acetonitrile solution of acridinium hydrochloride and an aqueous solution of Li-TCNQ and LiI being used. The black needles were obtained after a month. The crystals are triclinic. The crystal data are: $(C_{13}H_{10}N)^+(C_{12}H_4N_4)_2^-$, F. W. 588.6; $a=3.841(2)$, $b=13.018(6)$, $c=18.370$ (12) Å, $\alpha=114.32(5)$, $\beta=119.31(4)$, $\gamma=90.57(7)$, Space group, $P1$ or $P\bar{1}$; $U=703.5$ Å^3; $D_m=1.389$ g/cm^3, $D_x=1.389$ g/cm^3; $Z=1$

The intensity data were collected on an automated Rigaku four-circle diffractometer with Mo$K\alpha$ radiation monochromated by a graphite crystal. The $\omega-2\theta$ scan technique was employed. Among the 3149 accessible reflections ($2\theta\leqq55°$), 900 non-zero reflections were observed.

Structure Determination

The trial atomic coordinates were easily deduced from the three-dimensional Patterson synthesis and were refined isotropically by the block-diagonal least-squares method. The space group $P\bar{1}$ was assumed. The nine hydrogen atoms were found on the difference synthesis. Further refinements were carried out in anisotropic mode, however, the thermal parameters of the hydrogen atoms were assumed to be isotropic. The R-value converged to 0.087. The shifts of the parameters were about one fifth of their standard deviations. The weighting scheme adopted was: $w=1$ for $|F_o|\geq5.5$ and $w=0.32$ for $|F_o|<5.5$. The atomic scattering factors were taken from International Tables for X-ray Crystallography.[5] Because the orientation of ARD is disordered, the atomic scattering factor of CN(Table 1) was assumed to be $(f_C+f_N)/2$.

The final positional and thermal parameters are listed in Table 1. The calculated structure amplitudes are compared with the observed values in Table 2.*

Description of the Structure and Discussion

An ARD cation lie at (0,1/2,0) whose site symmetry is $\bar{1}$. Therefore, the orientation of ARD must be disordered because ARD is not centrosymmetric. Similar orientational disorder of cations has been frequently observed in the crystals of highly conducting salts(NMP–TCNQ[6] and Q(TCNQ)$_2$[7]). Fig. 1 shows that TCNQ and ARD are stacked along the a axis to form infinite columns. Each column of cations is surrounded by six columns of TCNQ as found in the crystals of Q(TCNQ)$_2$, which is a so-called complex salt (TCNQ/cation=2). The intermolecular distances of TCNQ and ARD are 3.246 and 3.418 Å, respectively. The least-squares planes and the displacement of the atoms from them are listed in Table 3. The mode of overlap of TCNQ is ring-external bond type as illustrated in Fig. 2. The similar type of overlapping of TCNQ is also found in NMP–TCNQ, Q(TCNQ)$_2$, Rb–TCNQ II,[8] ditoluenechromium (TCNQ)$_2$[9] and TTF–TCNQ[10]. All of them contain columns of monadic units of TCNQ, which indicates that this type of overlapping is common to the salts with monadic units of TCNQ. Short intermolecular contacts are listed in Table 4. A close approach distance of 3.15 Å occurs between the nitrogen atom of

* Table 2 have been deposited with the Chemical Society of Japan (Document No. 7413).

TABLE 1. ATOMIC PARAMETERS

Positional and thermal parameters of the non-hydrogen atoms, with their standard deviations in parantheses. The B_{ij}'s are defined by:

$$\exp[-(h^2B_{11}+k^2B_{22}+l^2B_{33}+2hkB_{12}+2hlB_{13}+2klB_{23})]$$

	x $\times 10^3$	y $\times 10^4$	z $\times 10^4$	B_{11} $\times 10^4$	B_{22} $\times 10^4$	B_{33} $\times 10^4$	B_{12} $\times 10^3$	B_{13} $\times 10^3$	B_{23} $\times 10^4$
C(1)	−415(3)	2879(9)	636(7)	63(11)	65(9)	48(7)	5(3)	10(2)	32(7)
C(2)	−217(3)	2269(8)	1134(7)	82(12)	41(8)	46(6)	4(3)	9(2)	22(6)
C(3)	173(3)	2783(8)	1941(7)	64(11)	57(9)	49(7)	2(3)	5(2)	36(7)
C(4)	358(3)	3984(8)	2330(7)	59(11)	54(8)	40(6)	2(2)	5(2)	26(6)
C(5)	157(3)	4603(8)	1840(7)	87(12)	47(9)	54(7)	3(3)	9(2)	31(7)
C(6)	−229(3)	4073(8)	1027(7)	88(12)	57(9)	54(7)	7(3)	11(3)	34(7)
C(7)	−828(3)	2336(9)	−209(7)	88(13)	67(9)	48(7)	7(3)	11(3)	34(7)
C(8)	760(3)	4528(8)	3165(7)	115(14)	47(8)	50(7)	7(3)	12(3)	34(7)
C(9)	−1035(3)	1149(8)	−623(7)	69(11)	60(8)	31(6)	5(3)	6(2)	23(6)
C(10)	−1045(3)	2924(9)	−717(7)	86(12)	57(9)	43(6)	4(3)	6(2)	25(7)
C(11)	977(3)	3967(9)	3698(7)	85(13)	56(10)	53(7)	1(3)	8(3)	20(7)
C(12)	966(3)	5699(9)	3538(7)	82(12)	61(9)	39(6)	3(3)	7(3)	24(7)
C(13)	−204(3)	578(8)	4478(7)	84(12)	62(9)	41(6)	10(3)	12(2)	30(7)
C(14)	−401(3)	1182(10)	3971(8)	110(14)	84(11)	58(7)	11(3)	17(3)	43(8)
C(15)	−776(3)	564(10)	3110(8)	146(17)	113(13)	62(8)	19(3)	19(3)	58(9)
C(16)	−934(3)	−638(10)	2732(8)	127(16)	90(12)	49(8)	7(3)	11(3)	23(8)
C(17)	−755(3)	−1238(9)	3216(7)	82(13)	82(11)	40(7)	3(3)	6(3)	25(8)
C(18)	−369(3)	−615(8)	4130(7)	75(12)	57(9)	47(6)	4(3)	14(2)	25(6)
N(1)	−1192(3)	181(8)	−982(6)	130(13)	73(9)	54(6)	0(3)	4(2)	29(7)
N(2)	−1221(3)	3410(8)	−1107(7)	132(13)	99(10)	68(7)	9(3)	10(3)	54(7)
N(3)	1141(3)	3498(8)	4128(7)	144(14)	91(10)	73(7)	2(3)	2(3)	51(7)
N(4)	1131(3)	6634(7)	3809(6)	163(15)	40(7)	40(6)	−4(3)	3(3)	13(6)
CN	175(3)	1157(7)	5357(6)	85(11)	47(7)	49(6)	4(3)	10(2)	30(6)

Positional parameters of the hydrogen atoms ($\times 10^3$)
The mean isotropic temperature factor is 1.3 Å^2.

	x	y	z		x	y	z
H(1)	−328(23)	144(7)	82(5)	H(6)	−891(27)	107(8)	279(6)
H(2)	304(24)	221(7)	218(5)	H(7)	−1251(34)	−88(10)	232(7)
H(3)	256(24)	542(7)	208(5)	H(8)	−851(24)	298(5)	298(5)
H(4)	−393(23)	449(7)	72(5)	H(9)	264(23)	196(7)	554(5)
H(5)	−270(29)	218(8)	430(7)				

TABLE 3. LEAST-SQUARES PLANES

Direction cosines of the normal of the plane with respect to:

		a		b		c
TCNQ		0.8453		−0.0539		−0.5315
ARD		0.8899		−0.0325		−0.4550
Deviation (Å)						
TCNQ	C(1)	0.03	C(2)	−0.00	C(3)	0.04
	C(4)	−0.03	C(5)	−0.01	C(6)	−0.03
	C(7)	−0.02	C(8)	0.01	C(9)	0.01
	C(10)	−0.03	C(11)	−0.03	N(1)	0.10
	N(2)	−0.07	N(3)	−0.09	N(4)	0.10
ARD	C(13)	−0.01	C(14)	0.01	C(15)	−0.03
	C(16)	0.03	C(17)	−0.01	C(18)	−0.01
	CN	0.01				

TABLE 4. INTERATOMIC DISTANCES

(i)	x	y	z	(ii)	$2-x$	$1-y$	$1-z$
(iii)	$-1-x$	$-y$	$-z$	(iv)	$-1+x$	y	z
(v)	$-2+x$	y	z	(vi)	$1-x$	$1-y$	$1-z$

Atom in unit (i)	To atom	In unit	d (Å)
N(4)	CN	ii	3.15
N(4)	H(9)	ii	2.36
N(1)	H(2)	iii	2.85
C(2)	C(3)	iv	3.28
C(4)	C(8)	iv	3.27
C(5)	C(12)	iv	3.30
C(6)	C(5)	iv	3.30
C(7)	C(1)	iv	3.25
H(5)	N(3)	v	2.83
N(4)	CN	vi	3.19
N(4)	H(9)	vi	2.66

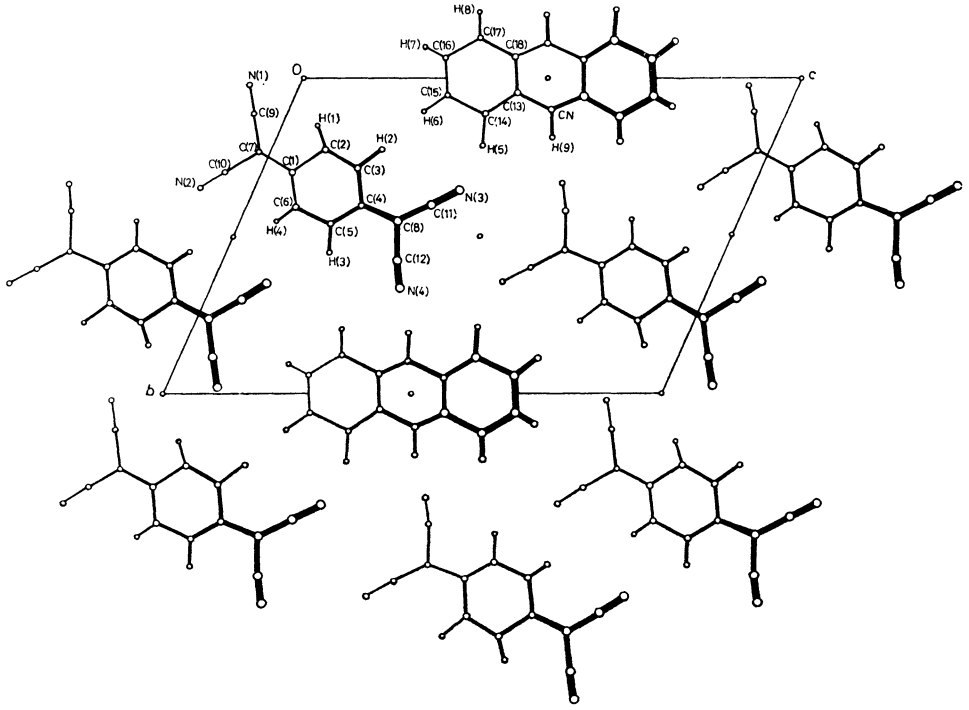

Fig. 1. The structure viewed along the *a* axis.

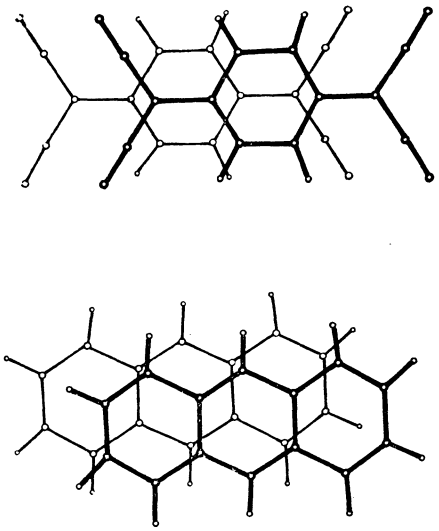

Fig. 2. Nearest neighbor overlap of TCNQ and that of ARD.

the cyano group of TCNQ and the CN atom(Table 1) of ARD cation. This indicates the possibility of the existence of the hydrogen bond of N–H···N type. Similar contact has been observed in the crystals of $Q(TCNQ)_2$ (3.13 Å).

TCNQ is almost planar but the cyano groups are rotated by about 2.4° around C=C bond from the molecular plane. Interplanar distance of ARD is approximately equal to the normal van der Waals distance.

The bond lengths and angles are shown in Fig. 3. The molecular geometry of TCNQ is that of $TCNQ^{-1/2}$ because only one TCNQ is crystallographycally independent. However, it dose not seem to be practicable to compare the bond lengths with those of $TCNQ^0$ and $TCNQ^-$ because of their large standard deviations.[11] Some rigid-body parameters are given in

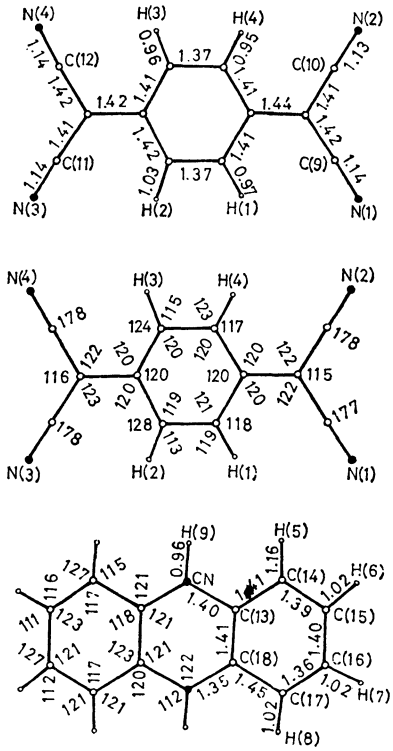

Fig. 3. Bond lengths (Å) and angles (°).
Estimated standard deviations for C-C(N) and C(N)-H bonds are about 0.018 and 0.10 Å, respectively. Those for C-C(N)-C(N) and C-C(N)-H angles are 1.1° and 5°, respectively.

TABLE 5. RIGID-BODY PARAMETERS OF TCNQ

Principal axes in the form: **La+Mb+Nc**

axis	L	M	N
1	0.2808	0.0391	0.0600
2	0.0045	−0.0737	0.0050
3	−0.1308	0.0268	0.0378

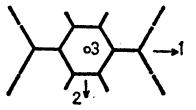

Molecular vibrational tensors

$$\mathbf{T}\times 10^4/\text{419}\quad \begin{pmatrix} 8 & -19 \\ 280 & 7 \\ & 404 \end{pmatrix}\ \text{Å}^2 \qquad \boldsymbol{\omega}\times 10/\text{465}\quad \begin{pmatrix} -14 & 10 \\ 20 & 7 \\ & 29 \end{pmatrix}\ \text{deg}^2$$

Principal axes of the **T** and $\boldsymbol{\omega}$ tensors relative to the molecular axes

R.m.s. amplitude	Direction cosines		
0.17 Å	−0.063	0.996	−0.064
0.20	−0.555	−0.088	−0.829
0.21	0.831	0.016	−0.556
1.2°	0.038	0.874	−0.485
1.8	0.003	−0.485	−0.874
6.8	0.999	−0.032	0.021

TABLE 6. INTERMOLECULAR DISTANCES AND THE TEMPERATURES SHOWING THE MAXIMUM ELECTRICAL CONDUCTIVITIES OF SOME HIGHLY CONDUCTING TCNQ SALTS

	intermolecular distance		$T^{2-4)}$
	TCNQ	cation	
TTF-TCNQ[10]	3.17 Å	3.47 Å	60 K
NMP-TCNQ[6]	3.26	3.36	200
Q(TCNQ)$_2$[7]	3.22	3.50	240
ARD(TCNQ)$_2$	3.25	3.42	150

Table 5. Interplanar distances in columns of highly conducting salts are listed in Table 6.

Classification of Columnar Structures of TCNQ. The magnetic susceptibility of alkali metal–TCNQ can be understood on the basis of the one-dimensional band model.[12] The extraordinarily large conductivity of TTF–TCNQ seems to suggest that the band gap produced by the deformation of a linear chain of TCNQ is important for the electrical properties of this salt. Thus it may be useful to make an attempt to interpret the physical properties of TCNQ salts on the basis of one-dimensional band picture. Table 7 shows the relationship between the columnar structures and the electrical conductivities of some TCNQ salts of known crystal structure. The columns composed of monadic, diadic, triadic and tetradic units of TCNQ have been reported. The salts with triadic and diadic units are

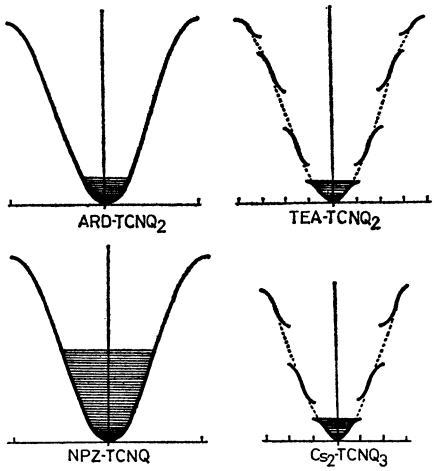

Fig. 4. Band structures for some types of TCNQ columns.

TABLE 7. COLUMNAR STRUCTURES AND ELECTRICAL RESISTIVITIES OF SOME TCNQ SALTS

	Cation : TCNQ	periodic unit	log $R^{a)}$	E_a(eV)[a]	Group
Rb-TCNQ I[b]	1:1	2	5	0.5	i
Cs_2TCNQ_3	2:3	3	4	0.3	i
$Morp_2TCNQ_3$	2:3	3	4	—	i
TEA(TCNQ)$_2$	1:2	4	1	0.13	ii
Meϕ_3P(TCNQ)$_2$	1:2	4	3	0.3	ii
Meϕ_3As(TCNQ)$_2$	1:2	4	3	0.3	ii
NproQ(TCNQ)$_2$	1:2	4	0	—	ii
Q(TCNQ)$_2$	1:2	1	−2	0.023[c]	iii
ARD(TCNQ)$_2$	1:2	1	−2	0.022[c]	iii
Rb-TCNQ II[b]	1:1	1	2	0.17	iii′[d]
NMP-TCNQ	1:1	1	−2	0.037[c]	iii
TTF-TCNQ	1:1	1	−4	0.006[c]	iii

Morp: Morpholinium, TEA: Triethylammonium, Meϕ_3P: Methyltriphenylphosphonium, Meϕ_3As: Methyltriphenyltriphenylarsonium, NproQ: *N*-(*n*-propyl)quinolinium.

a) Anisotropy of R(Ωcm at R.T.) is neglected. E_a is activation energy.[1-3,13,20] b) Rb-TCNQ I and RbTCNQ II are monoclinic and triclinic modification, respectively. c) Activation energy is that of low temperature region. d) The columnar structure of Rb-TCNQ II is similar to that of the salts of group (iii) but Rb-TCNQ I was not classified into group (iii) for convenience, because of its high resistivity. However, attention should be called to the fact that the conductivity of this modification is 10^3 times larger than that of the monoclinic modification.

low conductive(Cs_2TCNQ_3,[14] morpholinium$_2$TCNQ$_3$,[15] Rb-TCNQ I[16]). The salts with tetradic units are intermediately conductive(TEA(TCNQ)$_2$,[17] methyl triphenylphosphonium(TCNQ)$_2$, methyltriphenylarsonium(TCNQ)$_2$,[18] *N*-(*n*-propyl)quinolinium-(TCNQ)$_2$[19]). These facts indicate that the salts which contain two excess electrons in a repeating unit of TCNQ(2e/3TCNQ(Cs_2TCNQ_3), 2e/4TCNQ(TEA-(TCNQ)$_2$) are not highly conductive. Among these salts, those with tetradic units are more conductive. The high conductive salts are constructed from monadic units of TCNQ. The activation energy of the electrical conductivity of semiconductive region is less than 0.04 eV.[1-3,20] This small value suggests that the electrical conduction is not due to hopping process of excess electrons accompanying the deformation of TCNQ skeletons because such a process needs the activation energy more than 0.05 eV ($TCNQ_1^0 + TCNQ_2^- \rightarrow TCNQ_1^- + TCNQ_2^0, E > 0.05$ eV[17]) (a simple consideration is presented in Appendix). This seems to be one example showing the validity of the band picture. According to the band picture, the salts of groups (i) and (ii) (Table 7) are not metallic because they have filled bands (Fig. 4). Whereas, the salts of group (iii) with unfilled bands seem to be metallic and large electrical conductivity can be expected, which is consistent with the large conductivities of these salts. Thus, it may be useful to classify the columnar structure by the band picture.

Some Remarks on the Possibility of a Peierls Distortion of a Linear Chain of TCNQ. Although the columnar structures of the high conducting TCNQ salts indicate that these salts are metallic, they are semiconductive at low temperature. It may be of interest to see why they are not metallic at low temperature. The main reasons seem to be as follows:

(1) Owing to the Coulombic repulsion between two electrons on the same TCNQ site the antiferromagnetic state is considered to be more stable than the paramagnetic state, so that a simple band picture does not seem to be appropriate.[21] The metal-insulator transition of NMP–TCNQ has been analyzed in detail from this point of view.

(2) At low temperature, one-dimensional metallic lattice is unstable and the lattice seems to be distorted periodically with the wave vector of $2k_F$ (Peierls instability of one-dimensional lattice). Therefore, the metallic state may not be realized.[22]

A simple calculation was made in order to examine the possibility of a Peierls distortion of TCNQ columns.

If Peierls transition is realized at T_p, the following situations may result:

(1) At low temperature($T < T_p$), the electronic energy is lowered by the lattice distortion which produces the band gap at $k=k_F$.

(2) As temperature increases($T > T_p$), the free energy of the metallic state(columns with monadic units of TCNQ) becomes lower than that of semiconductive state(distorted columns) because the entropy of the metallic state increases. Accordingly the stabilization energy due to the lattice deformation will not be important.

Figure 5 shows a model of one-dimensional lattice

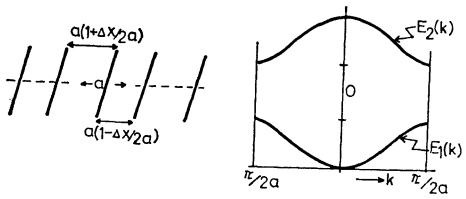

Fig. 5. A model of one-dimensional lattice of TCNQ and its split-band. a is assumed to be 3.25 Å.

of TCNQ. The two interplanar spacings $a(1+\Delta x/2a)$ and $a(1-\Delta x/2a)$ appear alternately. Each TCNQ is assumed to have one excess electron as in the case of NMP–TCNQ, which is usually called as a simple salt. Similar analysis may be applied to complex salts but the mode of alternation of lattice spacing will be more complicated. Δx is a parameter indicating the magnitude of the distortion of the lattice. Of course, real lattices are not one-dimensional, so that Δx may be regarded as a parameter representing a longitudinal modulation of a three-dimensional lattice. The tight-binding model of the band structure was adopted. The band structure is given by[12]

$$E_1(k) = -E_c(g^2+\cos^2 ak)$$
$$E_2(k) = -E_1(k) \quad (1)$$

where $E_c=2(h_1h_2)^{1/2}$ and $g=E_g/E_c$ ($E_g=|h_1|-|h_2|$, h_1 and h_2 are transfer integrals ($|h_1|>|h_2|$)). The transfer integral is estimated from Eq. (2).

$$h = h_0 \exp(-p\Delta x) \quad (2)$$

where $\Delta x=R-3.16$ and $h_0(=1878\ K)$ and $p(=3.91)$ are evaluated using the values employed by Vegter *et al.*[12] ($h(3.48\ Å)=538\ K$, $h(3.16\ Å)=1878\ K$). If $\Delta x \neq 0$, band gap is produced by lattice distortion at $k=k_F(=\pi/2a)$. The energy of lattice deformation is $\beta(\Delta x/2)^2/2$ per TCNQ(β=force const.). Free energy is written as

$$F = N\mu - k_BT\sum_\tau \log(1+\exp(-(\varepsilon_\tau-\mu)/k_BT) + N\beta(\Delta x/2)^2/2 \quad (3)$$

where $\varepsilon_\tau=E_1(k)$ or $E_2(k)$ and chemical potential μ is determined by,

$$N = \sum_\tau (\exp((\varepsilon_\tau-\mu)/k_BT)+1)^{-1} \quad (4)$$

By employing this simple model, Δx which minimizes free energy was obtained numerically at various temperatures. When $\beta=1.2\times10^5$ dyn/cm, the transition indicating Peierls instability was obtained at about 200 K(T_p). Considering the stiffness of the columns of TCNQ, this value does not seem to be unreasonable. The temperature dependence of Δx is shown in Fig. 6a. Δx decreases to zero as temperature increases up to T_p and it is zero when $T > T_p$. Figure 6b shows the specific heat of the electrons which is calculated by use of the values of Δx shown in Fig. 6a. A peak accompanied by Peierls instability is obtained around the temperature about 20 K below T_p. The heat of the transition is about 130 cal/mol. The magnetic susceptibility (Fig. 6c) is temperature independent above T_p($\chi=9.0\times10^{-5}$ emu), indicating the Pauli spin susceptibility.

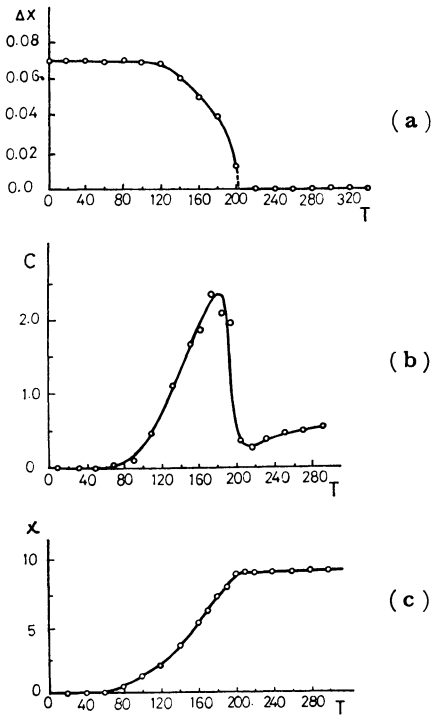

Fig. 6. (a) The temperature dependence of Δx(Å). (b) Specific heat. C is in $0.05k_B$ unit. (c) Magnetic susceptibility ($\chi \times 10^5$).

Thermal expansion of the intermolecular spacing was neglected in this model. Although this model seems to be oversimplified, it may be reasonable to consider that it shows the possibility of a Peierls distortion of high conducting TCNQ salts. Recently, Rice and Strässler have presented an interesting theory of Peierls distortion and Peierls soft mode of a quasi-one-dimensional band-conductor. Starting from a Fröhlich electron-phonon Hamiltonian, they show "how the giant Kohn anomaly in a higher-temperature metallic state can be the precusor of a second-order phase transition to a lower-temperature insulating phase (Peierls insulator)".[23] Zeller *et al.* showed that the evidence of Peierls instability or Kohn anomaly in one-dimensional conductors of type $K_2Pt(CN)_4Br_{0.30}\cdot xH_2O$.[24] The coherence length of the modulated chains is found to be larger than 400 Å. Anomaly in the longitudinal acoustic phonon branch of $K_2Pt(CN)_4Br_{0.3}\cdot 3H_2O$ was observed by inelastic neutron scattering.[25]

The calculations were performed on the HITAC 8700/8800 computer at the Computer Centre of Tokyo University.

The author would like to express his thanks to Professor Yoshihiko Saito for his keen interest and for his kind permission to use the four-circle diffractometer. He also thanks to Dr. Ichimin Shirotani for valuable discussions.

Appendix

The molecular geometry of TCNQ°(neutral molecule) is different from that of TCNQ$^-$.[11,26] The magnitude of the change in bond lengths corresponds to the change in their bond orders. It is the purpose of this Appendix to see a role of molecular deformation on a hopping motion of an excess electron TCNQ columns.

Table 8. Bond lengths and force constants

	TCNQ°	TCNQ$^-$	$\lvert\Delta r\rvert$	k[30]	m
1	1.344 Å	1.356 Å	0.012 Å	5.7 mdyn/Å	4
2	1.446	1.425	0.021	3.6	8
3	1.371	1.401	0.030	4.8	4
4	1.434	1.417	0.017	4.9	8
5	1.140	1.155	0.015	16.7	8

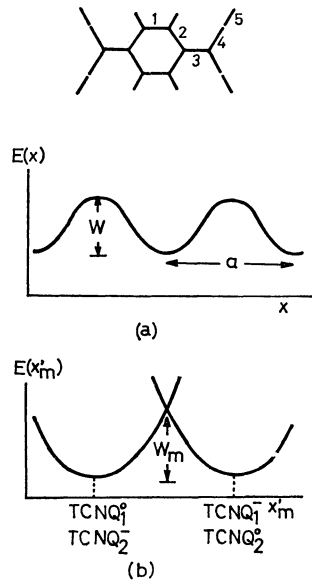

Fig. 7. (a) Potential energy-configuration diagram. (b) The deformation energy of TCNQs for one-electron transfer.

Because the frequency of hopping motion of an excess electron ($\nu_0 \simeq 10^{12}$ s^{-1})[27] is considered to be less than that of molecular vibrations ($\nu_m \simeq 10^{13}$ s^{-1}), the hopping motion of the excess electron may be accompanied by the molecular deformation. Consider an excess electron moving on an adiabatic potential surface $E(x)$ (see § 4 in Ref. 28). $E(x)$ is a periodic potential with a period of a Å. By a simple consideration, following equation can be obtained.[28,29]

$$\sigma = \nu_0 e^{-W/kT} Nne^2a^2/kT \qquad \text{(A1)}$$

where σ is the electrical conductivity, N is the number of chains of TCNQ per unit cross sectional area and n is the electron density on the chain. If $W=0$, Eq. (A1) is identical to that derived by Bloch *et al.* (Einstein equation).[27] σ is maximum when $T=W/k$ (Eq. (A1) is not accurate when $kT \geqq W$ but it may be useful for qualitative discussion). The activation energy may be written as

$$W = W_l + W_m, \qquad \text{(A2)}$$

where W_l and W_m are deformation energies due to lattice and molecular distortions, induced by the excess electron respectively. In most cases, W_m may be approximately equal to the energy of deformation of TCNQ and can be estimated using molecular geometries obtained by X-ray crystal structure analyses (Table 8 and Fig. 7)

$$W_m = \sum_i m_i k_i (\Delta r_i/2)^2/2 \qquad \text{(A3)}$$

where k_i is the force constant of the i-th bond, Δr_i is the change of bond length and m_i is the multiplicity of the i-th bond per

two TCNQs.

W_m is calculated to be 0.059 eV. Therefore, $W(=W_1+W_m)>W_m\simeq 0.06$ eV. Considering that W is larger than kT ($=0.025$ eV at R. T.), the molecular distortion seems to play important role when an excess electron moves between strongly localized states. Of course, the situation is more complicated in real crystals. Electron-electron interaction may be important. However, concerning the interaction between molecular vibrations and excess electrons, the situation would be similar to that of this simple model to some extent. From this point of view, it may be unlikely that the electric conduction of the highly conductive TCNQ salts is due to the simple hopping mechanism because the activation energies are less than 0.04 eV.[1-3,20]

References

1) L. B. Coleman, M. J. Cohen, D. J. Sandman, F. G. Yamagishi, A. F. Galito, and A. J. Heeger, *Solid State Column.*, **12**, 1125 (1973). J. Ferraris, D. O. Cowan, V. Walatka, and J. H. Perlstein, *J. Amer. Chem. Soc.*, **95**, 948 (1973). P. M. Chaikin, J. F. Kwak, T. E. Jones, A. F. Galito, and A. J. Heeger, *Phys. Rev. Lett.*, **31**, 601 (1973). J. Bardeen, *Solid State Commun.*, **13**, 357 (1973). A. A. Bright, A. F. Galito, and A. J. Heeger, *ibid.*, **13**, 943 (1973).
A. N. Bloch, J. F. Ferrais, D. O. Cowan, and T. O. Poehler, *ibid.*, **13**, 753 (1973). P. W. Anderson, P. A. Lee, and M. Saitoh, *ibid.*, **13**, 595 (1973). P. A. Lee, T. M. Rice, and P. W. Anderson, *Phys. Rev. Lett.*, **31**, 462 (1973).

2) A. J. Epstein, S. Etemad, A. F. Galito, and A. J. Heeger, *Phys. Rev., B*, **5**, 952 (1971). L. B. Coleman, J. A. Cohen, A. F. Galito, and A. J. Heeger, *ibid., B*, **7**, 2122 (1973).

3) V. Walatka and J. H. Perlstein, *Mol. Cryst. Liq. Cryst.*, **15**, 269 (1971).

4) L. I. Bravov, D. N. Fedutin, and I. F. Shchegolve, *Sov. Phys. JETP*, **32** 612 (1971).

5) "International Tables for X-ray Crystallography," (1962). Vol III, Birmingham: Kynoch Press. References therein.

6) C. J. Fritchie, *Acta Crystallogr.*, **20**, 892 (1966).

7) H. Kobayashi, F. Marumo and Y. Saito, *ibid., B*, **27**, 373 (1971).

8) I. Shirotani and H. Kobayashi, This Bulletin, **46**, 2595 (1973).

9) R. P., Shibaeva, L. O. Atovmyan, and M. N. Orfanova, *Chem. Commun.*, **1969**, 1494.

10) T. E. Philips, T. J. Kistenmacher, J. P. Ferrais and D. O. Cowan *ibid.*, **1973**, 471.

11) H. Kobayashi, This Bulletin, **46**, 2945 (1973).

12) J. G. Vegter, J. Kommandeur, and P. A. Fedders, *Phys. Rev., B*, **7**, 2929 (1973).

13) L. R. Melby, R. J. Harder, W. R. Hertler, W. Mahler, R. E. Benson, and W. E. Mochel, *J. Amer. Chem. Soc.*, **84**, 3374 (1962). W. J. Siemons, P. E. Biersted, and R. G. Kepler, *J. Chem. Phys.*, **39**, 3523 (1963).

14) C. J. Fritchie and P. Arthur, *Acta Crystallogr.*, **21**, 139 (1966).

15) T. Sundaresan and S. C. Wallwork, *ibid., B*, **28**, 491 (1972).

16) A. Hoekstra, T. Spoelder, and A. Vos, *ibid., B*, **28**, 14 (1972).

17) H. Kobayashi, Y. Ohashi, F. Muramo, and Y. Saito, *ibid., B*, **26** 459 (1970).

18) A. T. McPhail, G. M. Semeniuk, and D. B. Chesnut, *J. Chem. Soc., A*, **1971**, 2174.

19) T. Sundaresan nad S. C. Wallwork, *Acta Crystallogr., B* **28**, 1163 (1972).

20) I. F. Shchegolev, *Phys. Stat. Sol., A*, **12**, 9 (1972).

21) H. Shiba, *Bussei*, **13**, 615 (1972). D. Adler, *Solid State Phys.*, **21**, 1 (1968). B. Johansson and K. F. Berggren, *Phys. Rev.*, **181**, 855 (1969).

22) R. E. Peierls, "Quantum Theory of Solids," Oxford U. P., London (1955), D. Adler and H. Brooks, *Phys. Rev.*, **155**, 826 (1967).

23) M. J. Rice and S. Strässler, *Solid State Commun.*, **13**, 125 (1973).

24) R. Comes, M. Lambert, H. Launois, and H. R. Zeller, *Phys. Rev., B*, **8**, 571 (1973).

25) B. Renker, H. Rietschel, L. Pintschovius, W. Gläser, P. Brüesch, D. Kuse, and M. J. Rice, *Phys. Rev. Lett.*, **30**, 1144 (1973).

26) F. H. Herbstein, "Perspectives in Structural Chemistry," eds. J. D. Dunitz and J. A. Ibers, Vol. IV, (1971).

27) A. N. Bloch, R. B. Weisman, and C. M. Verma, *Phys. Rev. Lett.*, **28**, 753 (1972).

28) J. Yamashita and T. Kurosawa, *J. Phys. Soc. Japan*, **15**, 802 (1960).

29) H. Fröhlich, "Theory of Dielectrics," Clarendon Press, Oxford (1958).

30) T. Takenaka, General Symposium on Molecular Structure and Spectroscopy, Fukuoka, Oct. 1969.